U.S. Department of Energy
2019 Collegiate Wind Competition

University of Wisconsin-Madison

Electrical Sub-team Fotios Emery *(WiscWind Team Lead* | *EE Team Lead)* Hongyi Gu Mitchell Kuhlman Chemutai Shiow Davis Wade Michael Craney Justin Casselton	**Mechanical Sub-team** Jacob Colvis *(ME Team Lead)* Denzel Bibbs Jacob Free Kelsey Hacker Alex Hotz Anson Liow Yi Liu Tom Vandenburg Devin Welch	**Siting Sub-team** Joe Brunner *(Siting Team Lead)* Jake Bever Aaron VanDeurzen **Principal Investigator** Scott Williams **Contact** spwilliams@wisc.edu

Table of Contents

Executive Summary

WiscWind is an interdisciplinary engineering student organization competing in the U.S. Department of Energy 2019 Collegiate Wind Competition (CWC), giving students real-world experience in the growing renewable energy industry. The mechanical and electrical sub-teams are tasked with designing and fabricating a wind-driven power system that maximizes power generation. This turbine will be subjected to five tests outlined in the competition's rules and regulations.

The mechanical sub-team completed research on last year's design to improve competition results from the 2018 competition. The major tasks this year have included, but are not limited to, beginning rework on the blade design, implementation of the passive pitch control, and further research for the pitch and yaw controls. All of these factors have been worked on to improve the mechanical efficiency of the turbine. This will allow a greater speed of the shaft for a given wind speed, which creates a greater power output. With a greater power output, the team will score higher marks in the categories that will be judged at the CWC. The fall semester was dedicated to further research, preliminary testing and beginning the implementation of the passive pitch control; the spring semester was comprise of new fabrication, further re-work of design, and additional testing.

The electrical sub-team focused converting the mechanical energy captured by the wind into electrical energy is accomplished with a custom made three phase axial flux generator. Power electronic circuits control high efficiency AC to DC conversion, electrical noise suppression, emergency load disconnected, and emergency braking using an Arduino microcontroller and a combination of hand built and off the shelf circuitry. The fall semester was dedicated to reworking and refitting the generator. The team's main focus was on the wires carrying the output phases of each stator. These wires were attached more securely to their respective stator and a new case for the generator was designed which exerted less pressure on them. The spring semester was dedicated to the rated voltage output and safety tasks of the competition. These tasks will be achieved through our power output board and our safety module. Our safety module consists of the safety circuits and the control logics that will account for two different situations: disconnect of load, and manual or emergency shutdown.

Our mechanical and electrical designs have been an iterative process. All parts will be purchased, machined, and assembled by members of the team. Most components have been tested individually, if possible, before running final tests on the wind turbine. With scheduled wind tunnel testing about every month, we have had the opportunity to verify our design choices as well as optimize our turbine from last year. The combined properties of the wind turbine will withstand all competition requirements and excel in power generation and performance.

Introduction

WiscWind's development and design for the prototype turbine focused on optimizing performance at cut-in and low wind speeds and maximizing the turbine power output over all wind speeds. This is achieved through several power saving features such as passive yaw and pitch control, blades optimized for low speed efficiency, and a generator design which eliminated cogging torque. The mechanical design also focused on structural integrity and advanced composites manufacturing practices. Converting the mechanical energy captured by the wind into electrical energy is accomplished with a custom made three-phase axial flux generator. Power electronics circuits control AC to DC conversion, power regulation, and emergency braking. The technology from the development of the prototype turbine will be integral to the development of the full-scale market turbine.

Mechanical

Mechanical Design Objectives

WiscWind's top priorities in its design were achieving both a low cut-in speed and stable power curve. In order to meet these criteria, the blades and control systems have been designed with the balance of these requirements in mind. The blade geometry controls the cut-in speed of the wind turbine and the control systems ensure that the power curve is stable and predictable across a wide range of wind speeds. As this is a small-scale wind turbine, both the pitch and yaw control were designed to be operated passively, so that the maximum amount of energy could be extracted. The prototype blades were designed and later redesigned with the intention of striking a balance between the cut-in speed and power curve objectives. While there are many other subsystems of the wind turbine including the nacelle and tower subassemblies, they do not have as much of an impact on the desired performance abilities of the wind turbine as the blades and control systems. An assembly of our prototype wind turbine can be seen in Figure 1 below.

Figure 1. Full prototype turbine assembly in wind tunnel for testing.

The design objectives of the prototype were driven by the rules and regulations of the Collegiate Wind Competition. Three major criteria were considered in accordance with these regulations:

Size Constraints - The turbine must fit within a 45cm x 45cm x 45cm cube area centered 60 cm above the bottom of the wind tunnel.

Power Production – In order to maximize the points for power production, the turbine was designed with several key subassemblies. The passive pitch control mechanism allows the blades to perform at higher efficiency over a broad range of wind speeds. The direct drive axial flux generator further reduces mechanical losses by eliminating the need for a gearbox. The yaw system reduces the control system power consumption by acting passively.

Durability - The turbine must withstand 20 m/s wind, including various wind-speed profiles.

The design process of the prototype turbine is described below, beginning with preliminary airfoil selection and ending with the design of the nacelle. The full mechanical assembly can be referenced in Appendix B.

Blades

WiscWind's blade design focused on choosing the best airfoil shape and blade size for balancing a low cut-in speed with performance at higher speeds, as well as choosing fabrication-capable materials that are both inexpensive and durable. This process required use of multiple simulation programs and databases, as well as contact with on-campus resources.

Blade Design

Blades were designed in an iterative two-step process. First, XFOIL, an open-source airfoil analysis tool, was used to simulate flow over airfoil geometries at design conditions. An in-house MATLAB code was created to interface with XFOIL in order to simulate hundreds of airfoil shapes in sequence. The profile with the optimal lift to drag characteristics, NACA 3210, was chosen [1]. Next, the blade was designed based on the characteristics of the airfoil. 20 sections based on the NACA 3210 with varying thicknesses were modeled in QBlade, an open-source rotor design tool [2]. Using the Betz optimal propeller theory [3], the ideal chord and twist distribution was calculated. Simulations were then run in QBlade to determine the blade's power output at various tip-speed ratios (TSRs) to tune the design for optimal performance, as shown in Figure 2. Finally, the blades were manufactured and tested on the model turbine to compare with previous models. This process was iteratively repeated to converge to an optimal design.

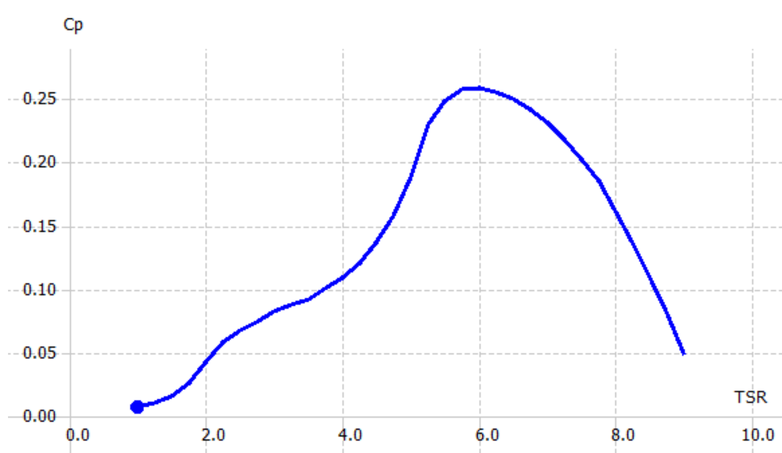

Figure 2. Graph of coefficient of performance vs. tip-speed ratio for NACA 3210.

Due to significant electromechanical losses, it was found that the turbine required a higher torque than desired to reach significant rotational speeds. Because of this, every blade we designed performed optimally at higher TSRs than testing produced. We also found that larger blades tended to perform better at lower TSRs, due to larger surface area to produce lift. Therefore, we chose to design the blade as large as reasonably possible without adding undue weight.

Manufacturing

Preliminary manufacturing of the blades consisted of 3D printing through the Makerspace on UW-Madison's campus and a third party, Midwest Prototyping. 3D printing may be used for mocking up pitch control components as well, and the final nacelle will likely by 3D-printed. Figures 2.1 and 2.2 show the final blade modeled in SOLIDWORKS and a 3D printed version respectively.

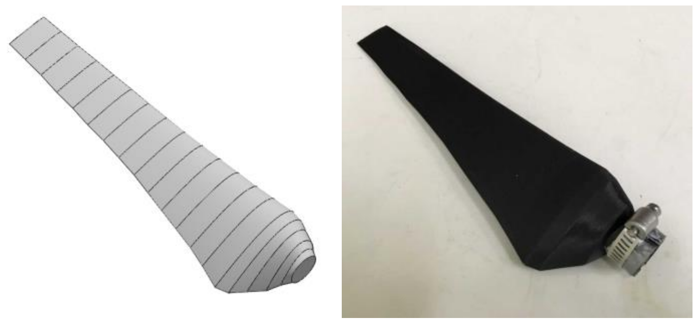

Figures 2.1 and 2.2. SOLIDWORKS model (left) and 3D printed blade (right).

Pitch Control

The objective of a pitch control system is to help provide an optimal power over a larger band of wind speeds. Most modern wind turbines incorporate active pitch control, typically electrically with motors or hydraulically [4]. While these systems have the advantage of being precise, they also require input power to rotate the blades. To get around this power input, the WiscWind team has decided to incorporate a passive pitch control that makes use of the rotational forces exerted on the turbine so as to avoid drawing power that is being generated.

WiscWind's pitch control system, shown in Figures 3 and 4 below, is inspired by a flyball governor system which relies on three masses rotating and moving outward from the main shaft from centrifugal force and springs to force masses back inward. Through a series of linkages, the masses are connected to an eccentric pivot, which rotates the blades. The angular position of the blades can rotate 40 degrees from their original position when the masses are extended.

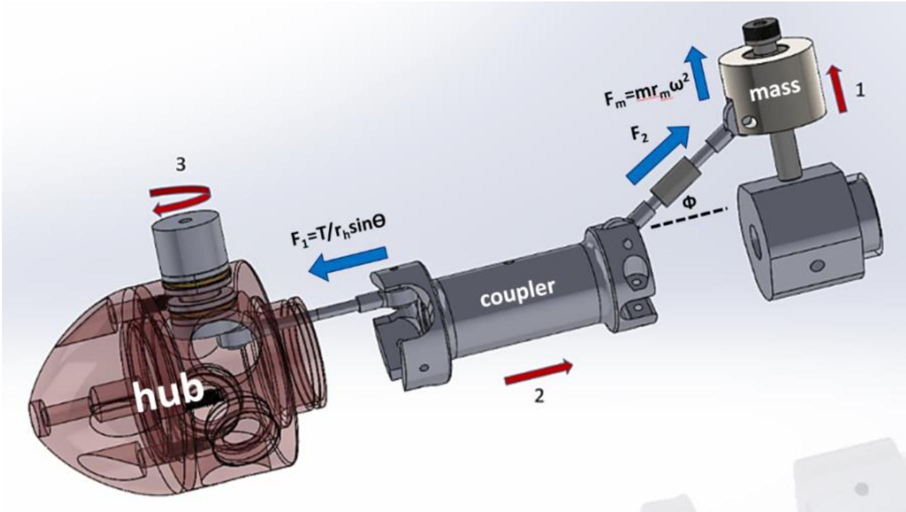

Figure 3. SolidWorks assembly showing equation of motion for pitch control.

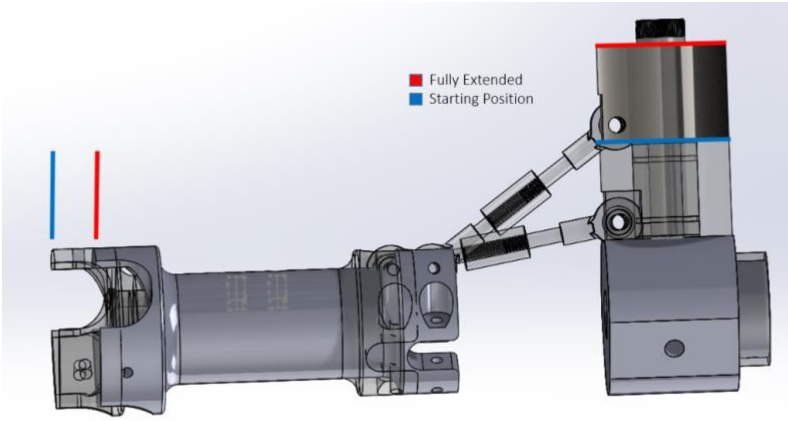

Figure 4. SolidWorks assembly detailing the pitch control system and the difference in positions.

As the system rotates, the mass moves outward from its starting position (see Figure 4) and the coupler at location 2 transfers the radial motion from the mass to translational motion applied to the base of the blades at position 3, represented in Equation 1. The blade is then rotated an angle of "Θ" from its starting position. Using the equations of motion for F_1, F_2, and F_m shown in the figure below, the pitch angle, Θ, was related to mass, m, and rotational speed, ω, by:

$$tan\phi \frac{T}{r_h sin\theta} = mr_m\omega^2 \tag{1}$$

where ϕ is the angle between the coupler and the mass linkage, T is the torque applied to the base of the blade, r_h is the distance between the linkage and blade base in the hub, and r_m is the distance between the axis of rotation and the centroid of the mass. This relationship was used to estimate values for the masses and spring constants to be used during testing. Once estimated values were obtained, several springs around the approximate stiffness were tested in order to home in on the optimal stiffness needed to move the blade to its desired position at each operating condition.

Yaw Control

The objective of the yaw control system is to orient the nacelle so that airflow is parallel to the rotor. This will maximize the kinetic energy of the wind that can be harnessed and converted to electrical energy. The nacelle rotates about vertical axis of the support tower. This allows the nacelle to shift orientation to the wind according to the direction of airflow.

Grid Fin Design

The WiscWind turbine in 2018 used box-shaped fins (i.e. grid fins) for yaw control. The design was inspired by the grid fins used on the SpaceX Falcon 9 rocket.

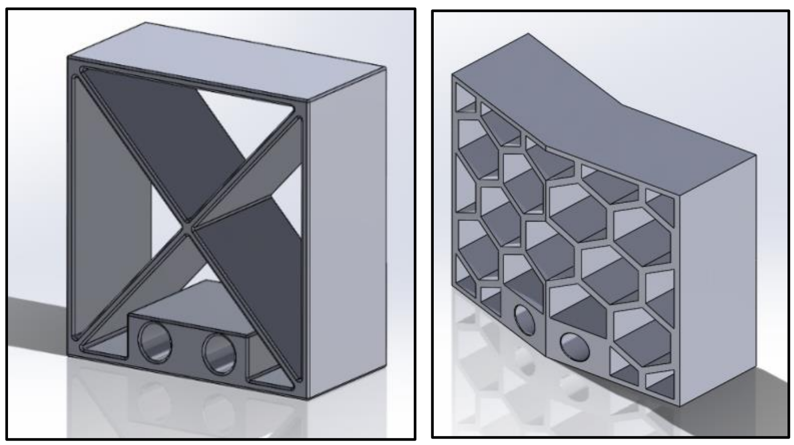

Figure 5.1 and 5.2. 2018 (left) and 2019 (right) WiscWind grid fins.

Figure 5.1 and 5.2 shows the 2018 and 2019 WiscWind grid fins. The surface area was increased from the 2018 grid fin using a hexagonal grid geometry. This was done to further increase the stability and response of the nacelle to directional changes in the wind. The 2019 grid fin also has a swept back by 10 degrees, which slightly improves aerodynamic efficiency [5].

Nacelle-Tower Coupler

In order to mitigate oscillatory behavior was the inclusion of large coupler which fits over the tower. The coupler is long enough to enclose multiple ball bearings held apart with aluminum spacers to provide more surface area and therefore stability. Figure 6.1 and 6.2 show multiple views of the coupler.

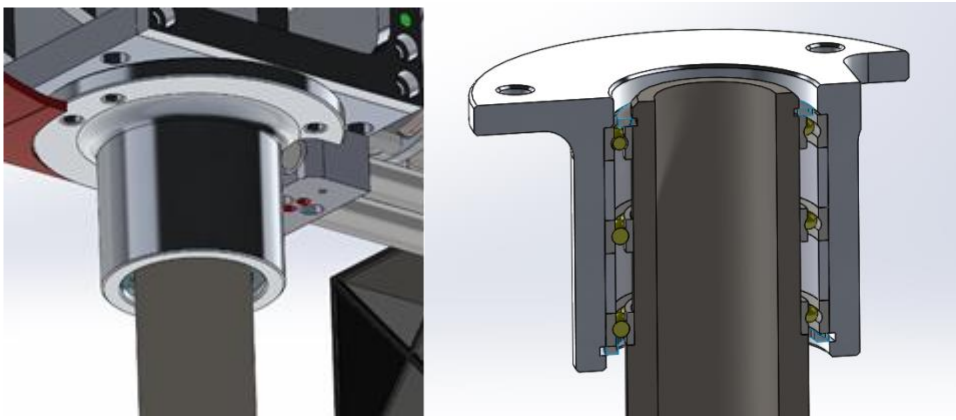

Figure 6.1 and 6.2. Coupler in the turbine assembly (left) and cross sectional view of the coupler (right).

Tower

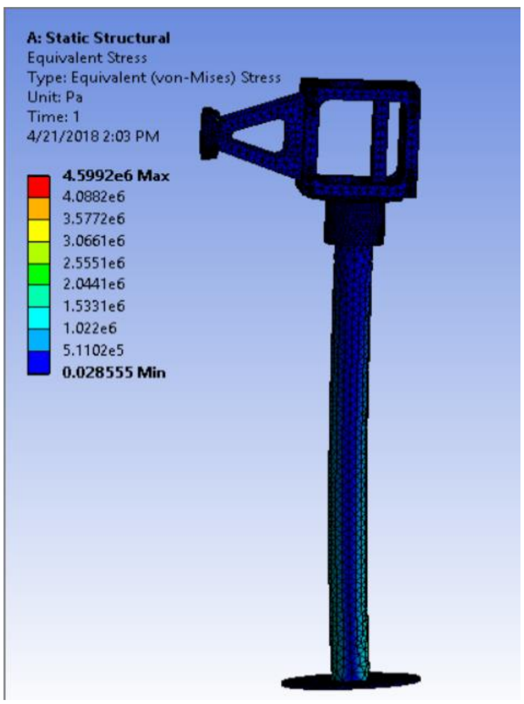

To maintain safe operation, the tower needs to be able to withstand all the loads placed upon it by the varying wind conditions. Worst-case bending loads were analyzed through ANSYS Mechanical by modeling the maximum wind force and determining the deflection, stresses, and factor of safety present in the tower, seen in Figure 7. The minimum factor of safety for the assembly was 15. This indicates the team does not have to consider failure of the tower through too high of wind speeds.

Figure 7. Main Mechanical housing under maximum loading conditions from high winds.

Nacelle

The design of WiscWind's nacelle was based around size constraints where the maximum size was constrained by the competition guidelines and the minimum size constrained by the number of components needed to be housed within the nacelle. Within these constraints, the nacelle was made as aerodynamic as possible to minimize disruptions to flow around the blades. The nacelle along with the full mechanical assembly can be seen in Appendix B.

Electromechanical

Electromechanical Design Objectives

The generator was designed to be fully modular to be able to adjust to the optimal operating points of the other turbine systems. The design was also focused on creating a machine which could be easily manufactured, assembled, and could be contained in one concise package for use on different turbine chassis in the future. In addition, we managed to make the generator more durable compared to previous years, particularly focusing on the wires carrying the output phases of each stator. These wires were attached more securely to their respective stator, and a new case for the generator was designed, which exerted less pressure on them.

Mechanical Design

Design Constraints

For the 2018 competition, the size of the generator was designed to have an outer diameter of 4 inches and an overall length of 5 inches. This was used as a starting point for the design since it was deemed large enough to effectively convert mechanical to electrical energy, yet small enough to not affect the aerodynamics around the nacelle of the turbine. As we began preparing for the 2019 competition, the dimensions of the generator were changed to better house the wires and alter the air gaps between the stators and the permanent magnets. This involved increasing the length to 5.25 inches and the diameter to 5.5 inches.

Stationary Components

The generator main body consists of a tube and two end caps. The end caps have shoulder features which ensure concentricity and parallelism for the bearings and rotating assembly. This allows the generator to achieve smooth and stable performance at high rotational speeds. The end caps are drawn together using three 4.5” long shoulder bolts. These shoulder bolts also provide mounting points for the stators inside the generator. One end cap is outfitted with a bolt hole pattern which allows the generator to be face mounted to the back of the turbine. The other end cap has mounting points for the circuit board, which sits at the back of the generator.

The stators proved to be one of the first manufacturing hurdles for the generator. The design uses a 3D-printed ring which provides structure for the stator before the coils have been cast in epoxy. The coils were placed inside the ring and connected together with a soldering iron. Finally, the stators were placed into a mold and filled with epoxy.

The stators were further improved this year. A great problem in last year’s competition was that the wires carrying the output phases of each stator would frequently break. First, we extended the leads coming out of each stator by soldering thin enameled copper wire to lengthen them. If a wire lead came out near or under a magnet, we used a soldering iron to dig a path for that wire through the stator’s epoxy and to the stator’s outer rim. Then all extended wire leads were secured by being submerged in epoxy and any hole made to the epoxy of the stator was filled and sanded off. Finally, the 6-pin output connector was connected to the longer enameled wire leads. Last year, the 6-pin output connector wires were a heavier gauge compared to the wire lead of the stator and as a result it would frequently rip off, especially when the case was compressing the wires. By connecting a more flexible lead to the generator’s stators, we were able to greatly reduce breakage and wire bending in a very small area. The wires are now allowed to flex over a longer distance.

Rotating Assembly

The rotating assembly consists of one main shaft and several rotors which are mounted to it. The rotors are connected to the shaft with a through pin, which provides both the rotational and translational constraints. The pin is then held in place with a collar to prevent it from sliding out while the generator is rotating.

This year new spacers were made for the generator as a response to a major problem with the previous generator design. When the three shoulder bolts securing the assembly were fully screwed down, the top magnet and top end plate would be squeezed together and the stators would rub against the magnets and as a result, the generator would not spin without applying a lot of torque. This "squeeze" could be fixed by only lightly tightening down the screws, however this caused the back of the generator to wobble and again was difficult to turn. We were able to overcome this problem by designing larger spacers that increased the air gaps between the stators and the magnets, which allowed the generator to be much easier to spin and cut in at a low wind speed. This introduced some electrical losses, but solved the issues of friction, hence improving overall efficiency.

Electrical Design

Design Constraints

The only major design constraint was the relationship between phase current and coil wire size. A wire size was chosen that provided adequate current overhead without the risk of burning out a coil or stator while remaining small enough to keep the coil fill factor high and overall generator efficiency high.

Coils

The number of coils for the generator was chosen as a baseline used last year. This number must conform to a specific ratio of coils to pole pairs, so setting the number coils to 12 locked in the number of magnets per rotor. The shape of the coils was chosen as trapezoidal, which most efficiently uses the space of the stator. The size of the wire used for the coils greatly affects their current carrying capacity. From simulations, it was estimated that the current output under normal conditions would be equal to or less than 1A. However, because the team is relying on the control circuit to electrodynamically brake the turbine by applying an extremely large load to the output of the generator, the current will be much higher during braking. Coil wire size affects the coil packing factor, which affects the efficiency of the generator. Large wire sizes reduce the packing efficiency, while smaller wires allow for tighter packed coils. A packing efficiency of 0.6 was assumed, which is typical for helically wound coils. Using the previous information and consideration, a coil wire size of 26 gauge was chosen. The final two parameters which were needed to fix the coils were found using EMWorks, a plugin for SOLIDWORKS, which provides tools that can simulate electromechanical machines. After the simulation was complete, the number of turns per coil was found to be 114 turns.

Coil Dimensions

Several different coil leg widths from 0.175 in to 0.3 in were simulated as shown in Figure 8. A coil leg width of 0.225 in was chosen because it maximized the output power while allowing for a larger coil form, which simplified manufacturing. Also, a few different coil widths from 0.075 in to 0.3 in were simulated as shown in Figure 9. A coil width of 0.225 in was chosen because it maximized the output power. This finalized the coil geometry and fix the number of turns to 114 turns per coil with our assumed coil fill factor.

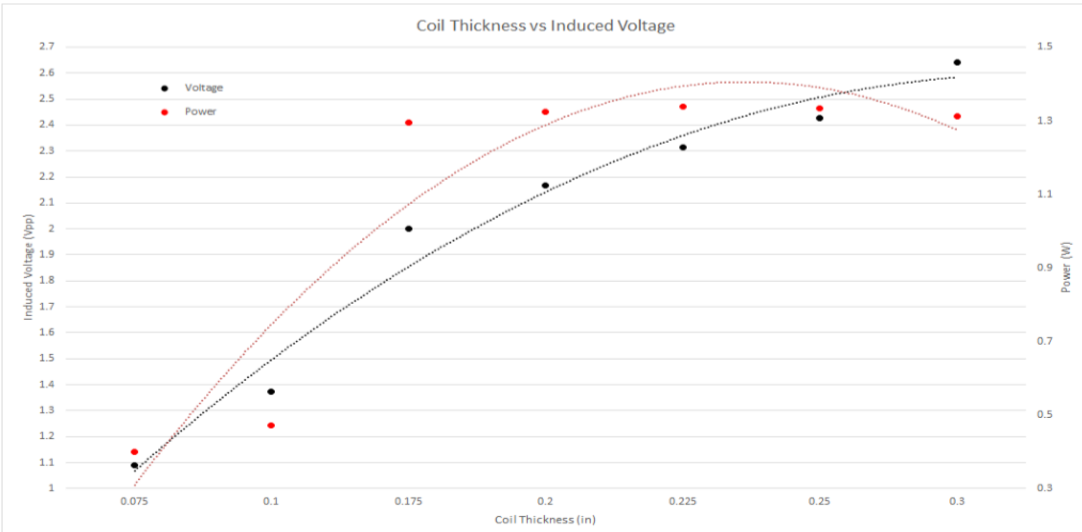

Figure 8. Induced Voltage vs Coil Thickness.

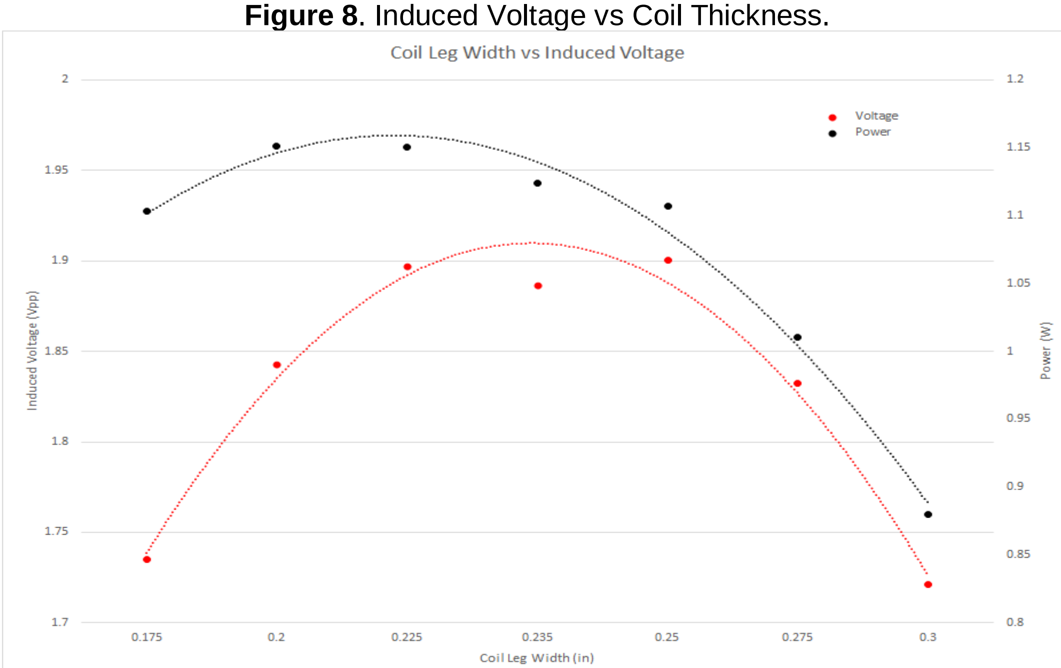

Figure 9. Induced Voltage vs. Coil Width.

Magnets

The shape of the magnets was set using the finalized shape of the coils. The inner and outer radius of the magnets were chosen to match the inner and outer radius of the empty area within the coils. The number of magnets was set to 9 using the 4:3 ratio of coils to magnets. The only other dimension that needed to be determined was the thickness of the magnets. Once again, EMWorks was used to determine the optimal magnet height.

Modular Design

Output of Generator Board

The circuit board located on the back of the generator combines the 9 total phases from the three separate "generators" (the three different 3-phase stator packs). In 2018, the team designed an output board that had the option to run in either a series or a parallel configuration. However, when we tested the output of generator board, we discovered that the 2018 design caused the generator to have shorted phases, which caused the turbine to be extremely difficult to turn. As a result, we decided to make a board that performs one of these functionalities. We first tried running the phases in parallel, which gave us lower voltage but higher current. However, at the output we were not getting enough power and as a result decided to run the generator in series getting more voltage and less current. This made our generator more efficient, as now the output voltage of our generator was in the range of voltages where our AC to DC rectification board was most efficient; thus we achieved higher efficiency.

The series PCB is illustrated in Figure 10, where each phase is represented by a battery for simplification reasons.

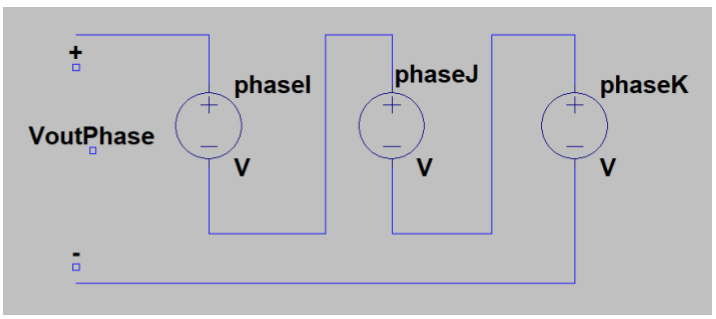

Figure 10. Schematic of Series PCB.

The output represents one phase out of three total output phases. Each of the three phases shown in Figure 10 that are in series (I, J, and K) would be, for example, all phase A's from each stator. This circuit is repeated three times on the PCB in order to add all three phases of each stator with each corresponding other two, resulting in three output phases, A, B, and C. This is shown in Figure 11.

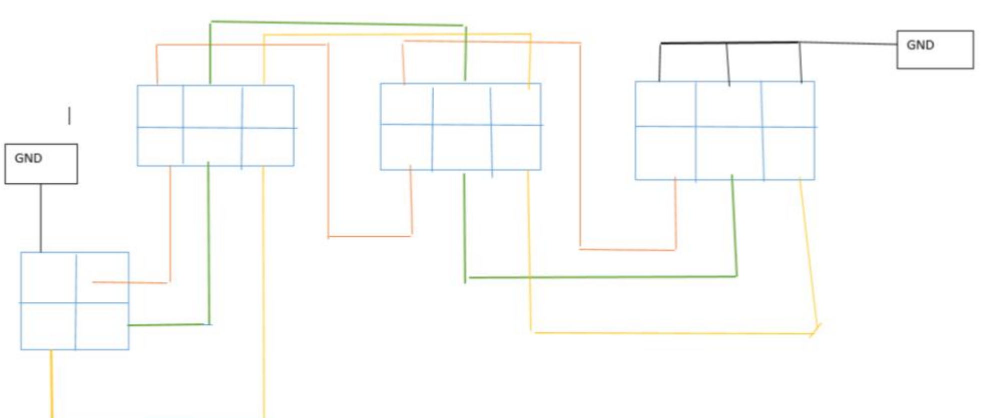

Figure 11. Output of generator board

The 2018 team used a conventional AC to DC three phase full bridge rectifier design that employs 6 IN5711 diodes to rectify the 3-phase voltage. This design introduces inefficiencies since the 6 diodes have forward voltage drops and consume some power. Therefore, this year's team decided to modify the previous design by using a low loss active 3-phase ideal diode bridge rectifier reference design. We are using the Linear Technology DC2465 board. On the board, there are three LT4320 IC's, which are ideal diode bridge controllers that drive six low loss N-channel MOSFETs to tell when they are on and off. The FETs are used as switching regulators, which turn on automatically without any voltage drops. This design dramatically reduces power and voltage losses. It enables the overall system to be specified to operate with a smaller, more cost-effective power supply due to the enhanced power efficiency. Low voltage applications benefit from the extra margin afforded by saving the two diode drops inherent in diode bridges. Compared to traditional approaches, the MOSFET bridge enables a rectifier design that is highly space- and power-efficient. Filtering will be done with a simple RC low pass filter on the output of the AC to DC converter, with a resistor value of 160 ohms, and a capacitance of 10 uF, which should give us a center frequency of 100Hz.

Safety Module

The safety module of our design considers two different situations: disconnect of load, and manual or emergency shutdown. This module consists of the safety circuits and the control logics. A diagram of the final design circuit can be found in Appendix A.

The safety circuits consist of the same two submodules of circuits and electronic components. The first submodule connects to the output of phase A and phase B, and the second submodule connects to phase B and phase C. Each submodule has a latching relay controlled by a 5V pulse signal input. The pulse signal is generated by control logic written in Arduino. A pulse signal at wire OFF would switch the state of the relay from on to off, and a pulse signal at wire ON would switch the state of the relay from off to on. Thus, by specifying the pulse signals at the ON wire and OFF wire, we can let the circuit path across the relay to switch between open circuit and closed circuit. During open circuit, the low impedance/high load resistor is disconnected and the turbine operates normally. During closed circuit, the circuit applies a very large load/small resistance between the phases. This causes a very large load to be present between phase A and phase B, and between phase B and phase C. The torque of the rotor is increased greatly to the point of almost stopping, and the generator power is transferred to the resistors in the safety circuits without transferring to the load. The wind turbine brakes and stops if the relay is maintained closed.

The control logic is written in Arduino that takes multiple signals as inputs and determines whether a 5V pulse signal output needs to be sent to the safety circuits to toggle the state of the relay and activate or deactivate the safety circuits. The Arduino Uno board is connected to a push button for signaling manual emergency shutdown, a current sensor for sensing load disconnect, and the relays in the safety circuits for shutting the turbine. Its power pin is also connected to the regulated output of AC/DC to make sure the control logics are always working under its rated voltage. The control logics use finite state machine to represent the state transitions and outputs needed under various input conditions. Initially, the state is set to 'normally operating', and the relay is opened. When the push button is pressed, the state transitions to 'button pressed', and a pulse signal is outputted to the relay to close it and shut down the turbine. Only when the button is pressed again would the state transitions back to 'normally operating', and a pulse signal is outputted to the relay to open it and resume the turbine. Therefore, repeatedly pressing the push button switches the state between manual/emergency shutdown and normal operation. We also connect a current sensor in series with the load. At the state of 'normally operating', when the current sensor's current reading is 0 or close to zero, we can know that there exists an open circuit at the load and conclude that the load has been disconnected. The state transitions to 'load disconnect', and a pulse signal is outputted to the relay to close it and shut down the turbine. Only when the load is connected and the current reading becomes nonzero would the state transitions back to ‘normally operating’, and a pulse signal is outputted to the relay to open it and resume the turbine. The finite state machine diagram is shown in Figure 12. The Arduino codes can be accessed via the URL attached in Appendix A.

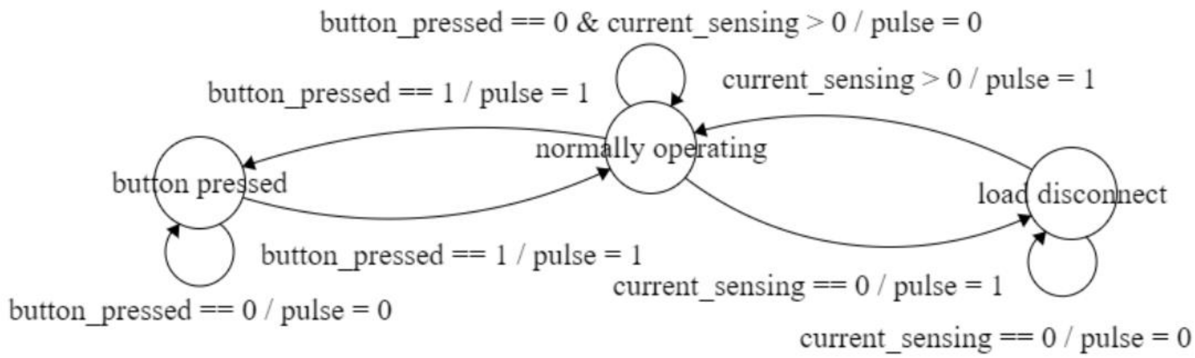

Figure 12. Finite State Machine of Safety board

Preceding the Arduino in the circuit is the DROK DC/DC Automatic Buck Boost Converter. This Buck Boost converter is used to supply a constant voltage to the Arduino in order to make sure it is always powered on and thus able to divert power to the safety system if required. It is rated for input voltages varying from 5V to 32V and is set to constantly output 12V for the Arduino. Table 1 below includes our results from voltage testing.

Table 1: DROK Voltage Regulation Testing Results

Input Voltage	Output Voltage
5.34 V	12.061 V
9.21 V	12.063 V
12.60 V	12.064 V
15.47 V	12.059 V
18.78 V	12.059 V

Voltage Regulation

The Voltage Regulator used is a TPS5516xEVM Single Inductor 1A Buck-Boost Evaluation Module. This regulator takes in anywhere from 2V to 36V, with a minimum supply of around 5.3V to start-up, and supplies a constant 5V at its output and a max current of 1 Amp. The in-house regulation design from 2018 (TPS5516) could not be used as it failed to provide a constant voltage during testing and was found to have been poorly implemented on the PCB. The traces were too thin for the expected high frequency input voltage and the traces between certain components were far apart. These long traces result in inconsistent voltage regulation being outputted as the regulator works due to constant feedback loops. With the spacing between components so large, by the time feedback is provided to the central unit the voltage at the input may be completely different so the feedback is no longer relevant. Regulators are very sensitive to part placement, line width, and trace lengths, all of which will be properly researched so an in-house regulator can be provided for future designs. Below, Table 2, is provided voltage regulation testing results on the TI regulator.

Table 2: TI Voltage Regulation Testing Results

Input Voltage	Output Voltage
5.40 V	4.986 V
10.13 V	4.985 V
12.57 V	4.986 V
12.86 V	4.985 V
12.35 V	4.985 V

The power will be delivered to the capacitor directly and stored. Our generator and voltage regulation system will maintain a voltage that is within the range of what the capacitor can handle.

Testing and Results

Optimization of Pitch Angle and Load Determination

In order to find the optimal pitch angle, we underwent testing in the wind tunnel to find the blade angle we will want in the competition's testing conditions. From this data in Figure 13.1, we found that the optimal angle was roughly 30 degrees. It should be noted that the cut-in speed was slightly lower than the first data point recorded in each position. Figure 13.2 shows the power output of the generator at the 30-degree pitch angle. The highest power output was found at a resistance of 300-Ohms, which will be the value used for our load in the competition.

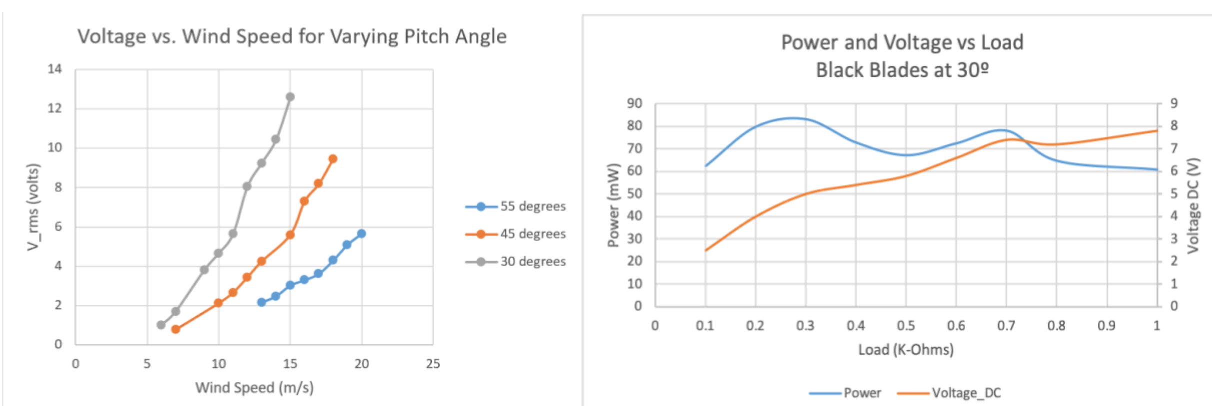

Figure 13.1 and 13.2. Experimental results for pitch angle optimization test.

Although the blade performed similarly to our assumptions in terms of blade pitch angle, we decided that even at the optimal blade pitch, our cut-in speeds were insufficient for competition and necessitated a rethinking of our blade design. Whereas our original blade design approach centered on maximizing efficiencies at higher speed, with the optimum occurring at rated power, the new design would place more emphasis on generating torque at low speed and cut-in. Using a similar process to that described in the 'Blade Design' section, this time with a lower optimal tip-speed ratio of 4, a new blade was decided upon. The new blade is based on the NACA 11XX airfoil series, which have less severe camber than the 32XX airfoils used originally. The new blade also has a substantially longer chord length and more twist than the original, which should provide better performance at low speeds at the expense of high speeds.

Characterization of C_p-TSR

Using the new blades at a pitch angle of 20 degrees, the turbine underwent testing to analyze its performance at various wind speed by connecting to the regulator with an additional resistance of 300 Ohms. Figure 14 shows the power coefficient vs. the turbine tip-speed ratio. From this characterization it is apparent that we are operating well below the design tip-speed ratio of 4 for competition wind speeds and the power coefficient suffers as a result.

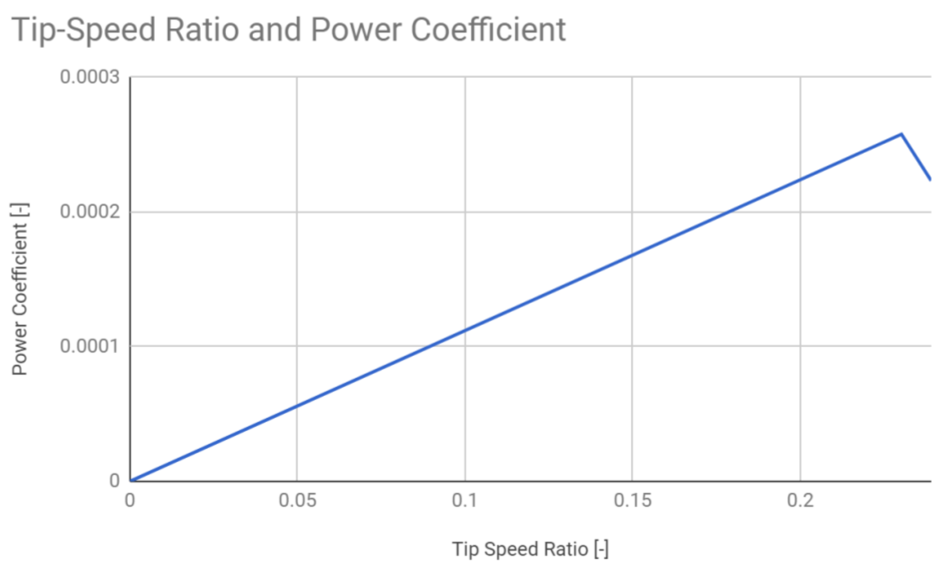

Figure 14. The turbine is operating below the designed tip-speed ratio.

From testing the pitch angle of the blades and the result on the power coefficient, we determine that for improved performance, it is necessary to either reduce the final load or redesign the blades to perform optimally at an even lower tip-speed ratio. These adjustments will be tested before the final competition.

Appendix A

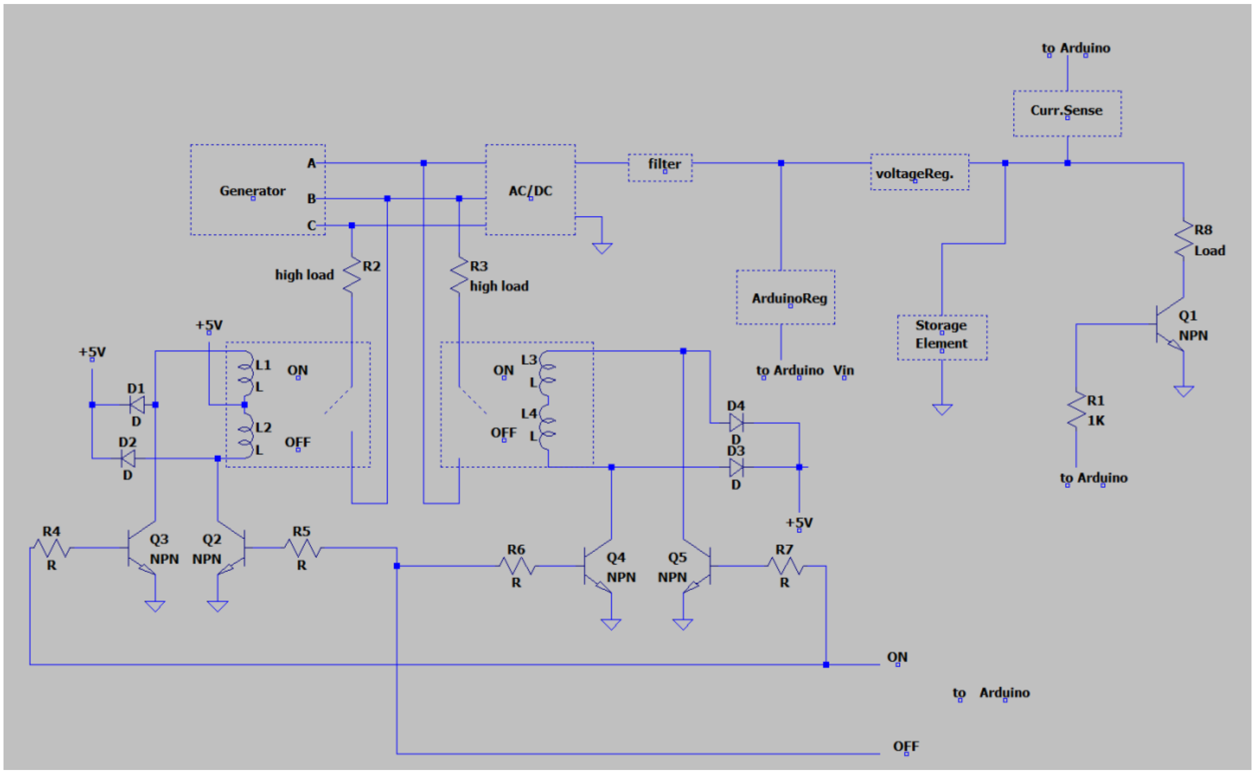

Figure A-1: Overall electrical design

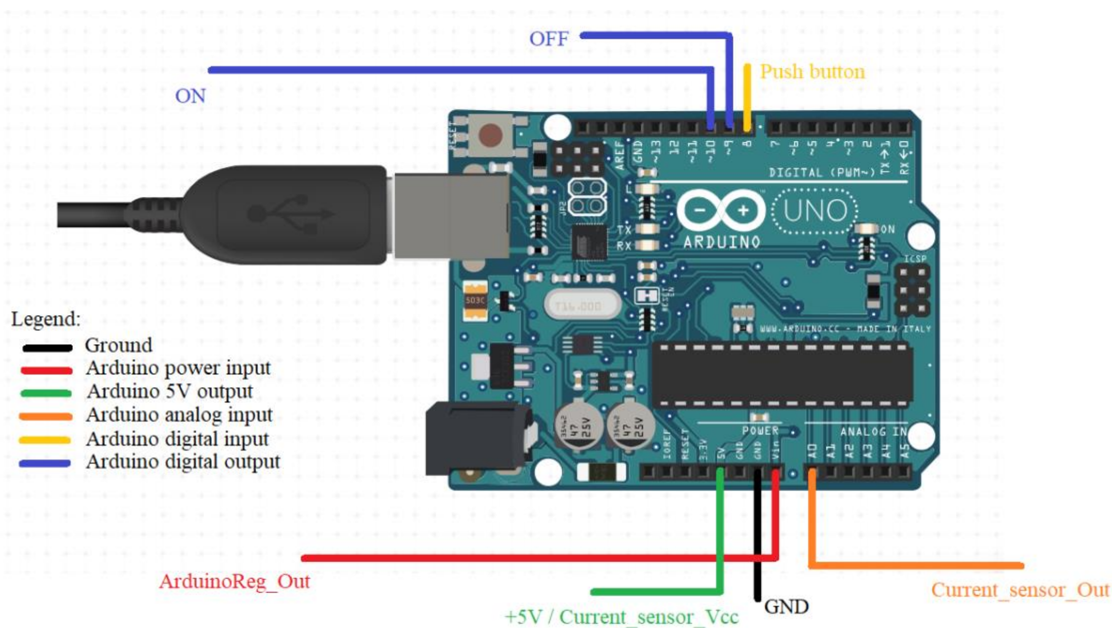

Figure A-2: Arduino wire connections. Arduino codes can be accessed via URL: https://github.com/HongyiGu/Wiscwind_safety_control

Appendix B

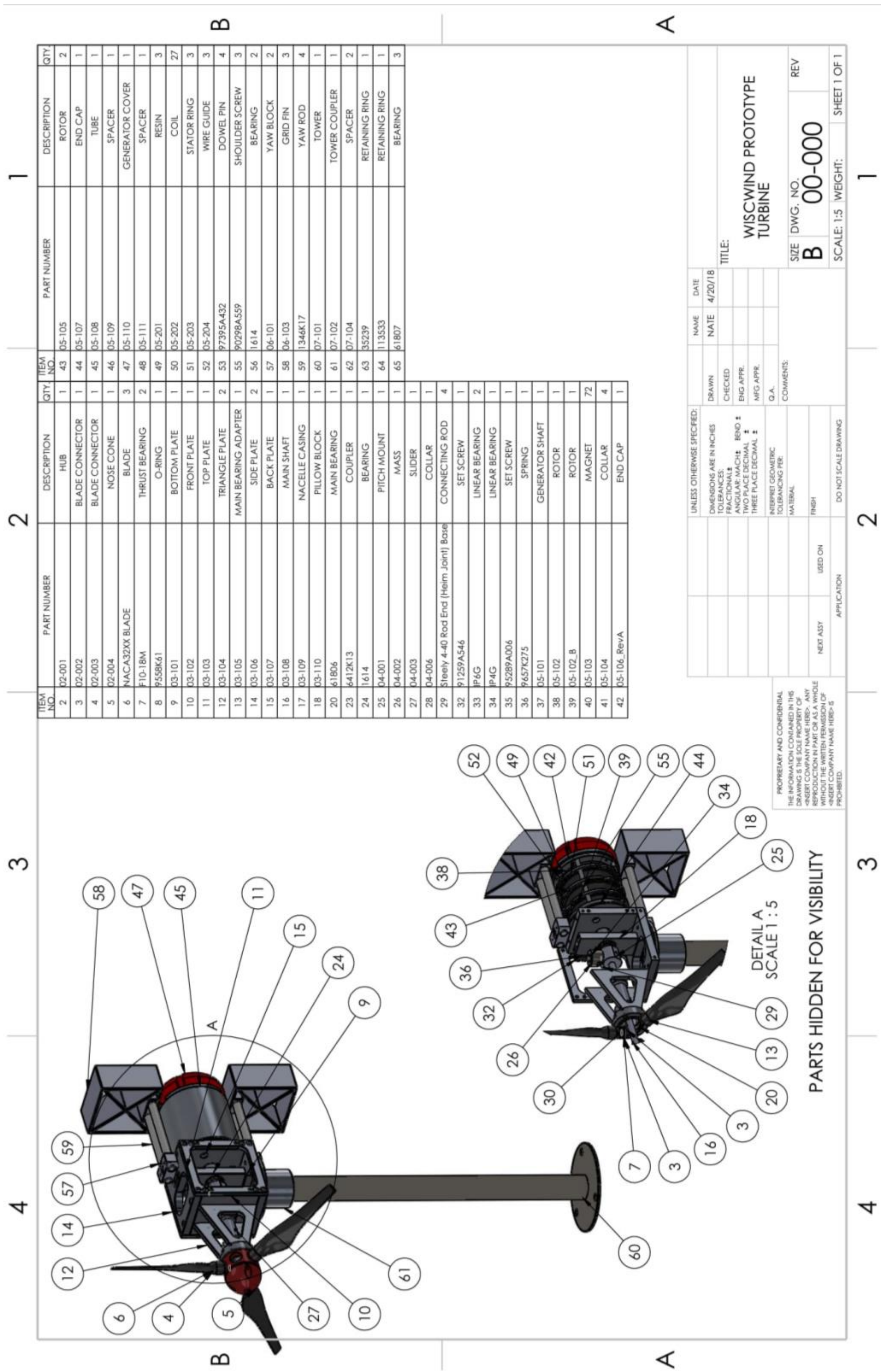

ITEM NO.	PART NUMBER	DESCRIPTION	QTY.
2	02-001	HUB	1
3	02-002	BLADE CONNECTOR	1
4	02-003	BLADE CONNECTOR	1
5	02-004	NOSE CONE	1
6	NACA32XX BLADE	BLADE	3
7	F10-18M	THRUST BEARING	2
8	9558K61	O-RING	1
9	03-101	BOTTOM PLATE	1
10	03-102	FRONT PLATE	1
11	03-103	TOP PLATE	1
12	03-104	TRIANGLE PLATE	2
13	03-105	MAIN BEARING ADAPTER	1
14	03-106	SIDE PLATE	2
15	03-107	BACK PLATE	1
16	03-108	MAIN SHAFT	1
17	03-109	NACELLE CASING	1
18	03-110	PILLOW BLOCK	1
20	61806	MAIN BEARING	1
23	6412K13	COUPLER	1
24	1614	BEARING	1
25	04-001	PITCH MOUNT	1
26	04-002	MASS	1
27	04-003	SLIDER	1
28	04-006	COLLAR	1
29	Steely 4-40 Rod End (Heim Joint) Base	CONNECTING ROD	4
32	91259A546	SET SCREW	1
33	P6G	LINEAR BEARING	2
34	P4G	LINEAR BEARING	1
35	95289A006	SET SCREW	1
36	9657K275	SPRING	1
37	05-101	GENERATOR SHAFT	1
38	05-102	ROTOR	1
39	05-102_B	ROTOR	1
40	05-103	MAGNET	72
41	05-104	COLLAR	4
42	05-106_RevA	END CAP	1

ITEM NO.	PART NUMBER	DESCRIPTION	QTY.
43	05-105	ROTOR	2
44	05-107	END CAP	1
45	05-108	TUBE	1
46	05-109	SPACER	1
47	05-110	GENERATOR COVER	1
48	05-111	SPACER	1
49	05-201	RESIN	3
50	05-202	COIL	27
51	05-203	STATOR RING	3
52	05-204	WIRE GUIDE	3
53	97395A432	DOWEL PIN	4
55	90298A559	SHOULDER SCREW	3
56	1614	BEARING	2
57	06-101	YAW BLOCK	2
58	06-103	GRID FIN	3
59	1346K17	YAW ROD	4
60	07-101	TOWER	1
61	07-102	TOWER COUPLER	1
62	07-104	SPACER	2
63	35239	RETAINING RING	1
64	113533	RETAINING RING	1
65	61807	BEARING	3

Figure B-1. Full Mechanical Assembly

References

[1] “XFOIL.” [Online]. Available: http://web.mit.edu/drela/Public/web/xfoil/. [Accessed: 22-Apr-2018].

[2] “QBlade.” [Online]. Available: http://www.q-blade.org/. [Accessed: 22-Apr-2018].

[3] Branlard, E. (2017). Betz Theory of Optimal Circulation. Research Topics in Wind Energy Wind Turbine Aerodynamics and Vorticity-Based Methods, 223-225. doi:10.1007/978-3-319-55164-7_12

[4] A. González-González, A. Jimenez Cortadi, D. Galar, and L. Ciani, “Condition monitoring of wind turbine pitch controller: A maintenance approach,” Measurement, vol. 123, pp. 80–93, Jul. 2018.

[5] G. A. Faza, H. Fadillah, F. Y. Silitonga, M. A. Moelyadi, in Journal of Physics: Conference Series (Institute of Physics Publishing, 2018), vol. 1005.